Published in final edited form as:
Biochim Biophys Acta. 2011 October ; 1811(10): 597–606. doi:10.1016/j.bbalip.2011.06.028.

Subcellular localization and regulation of StarD4 protein in macrophages and fibroblasts

Daniel Rodriguez-Agudo[1,+], **Maria Calderon-Dominguez**[1,#], **Shunlin Ren**[1], **Dalila Marques**[1], **Kaye Redford**[1], **Miguel Angel Medina-Torres**[#], **Phillip Hylemon**[3], **Gregorio Gil**[2], and **William M. Pandak**[1]

[1]Department of Medicine, Veterans Affairs Medical Center and Virginia Commonwealth University; Richmond, Virginia

[2]Department of Biochemistry and Molecular Biology, Veterans Affairs Medical Center and Virginia Commonwealth University; Richmond, Virginia

[3]Department of Microbiology/Immunology, Veterans Affairs Medical Center and Virginia Commonwealth University; Richmond, Virginia

[#]Department of Molecular Biology and Biochemistry, Universidad de Malaga, Spain

Abstract

StarD4 is a member of the StarD4 subfamily of START domain proteins with a characteristic lipid binding pocket specific for cholesterol. The objective of this study was to define StarD4 subcellular localization, regulation, and function. Immunobloting showed that StarD4 is highly expressed in the mouse fibroblast cell line 3T3-L1, in human THP-1 macrophages, Kupffer cells (liver macrophages), and hepatocytes. In 3T3-L1 cells and THP-1 macrophages, StarD4 protein appeared localized to the cytoplasm and the endoplasmic reticulum (ER). More specifically, in THP-1 macrophages StarD4 co-localized to areas of the ER enriched in Acyl-CoA:cholesterol acyltransferase-1 (ACAT-1), and was closely associated with budding lipid droplets. The addition of purified StarD4 recombinant protein to an *in vitro* assay increased ACAT activity 2-fold, indicating that StarD4 serves as a rate-limiting step in cholesteryl ester formation by delivering cholesterol to ACAT-1-enriched ER. In addition, StarD4 protein was found to be highly regulated and to redistribute in response to sterol levels. In summary, these observations, together with our previous findings demonstrating the ability of increased StarD4 expression to increase bile acid synthesis and cholesteryl ester formation, provide strong evidence for StarD4 as a highly regulated, non-vesicular, directional, intracellular transporter of cholesterol which plays a key role in the maintenance of intracellular cholesterol homeostasis.

Corresponding Author and Address: Dr. Daniel Rodriguez-Agudo, McGuire Veterans Affairs Medical Center & Virginia Commonwealth University, Medical College of Virginia, PO Box 980341, Richmond, VA 23298, Ph#: 804 828-3849, Fax#: 804 828-7430, drodriguezag@vcu.edu.

[+]Recipient of the American Heart Association Scientist Development grant. This work was supported by grants from the American Heart Association (0835197N), A.D. Williams fund, the Veterans Administration (Merit Review), and the National Institutes of Health (NIH 1RO1DK082464).

Keywords

Macrophages; Protein; Cholesterol; Metabolism; Steroidogenic Acute Regulatory Protein; Cholesterol Transporter; StAR; START domain

1. Introduction

Cholesterol is an important structural component of mammalian cell membranes, and serves as a precursor to bile acids (in the liver), steroid hormones (in the adrenal, testis and ovaries), and vitamin D. Homeostasis of cholesterol within the body is maintained through the coordinate regulation of its cellular mediated uptake, transport/trafficking, sorting, biosynthesis, storage (i.e. esterification), secretion, and catabolism to bile acids [1]. In recent years, a number of specialized non-vesicular lipid transporters that are part of the steroidogenic acute regulatory related lipid transfer (START) domain superfamily of proteins have been shown to be involved in the trafficking of cholesterol and other lipids between intracellular membranes [2–4].

All proteins with a START domain contain a similar binding pocket, where modifications determine ligand-binding specificity and function [5]. START domains are 200–210 amino acid motifs, which appear in a wide range of proteins, and have been implicated in several cellular functions including lipid transport and metabolism, signal transduction, and transcriptional regulation [2, 3, 6]. More specifically, a StarD4 subfamily of START domain proteins, that includes StarD4, StarD5 and StarD6, contains 205–233 amino acid residues and shares 26–32% identity [7]. StarD5 has been shown *in vitro* to bind cholesterol and 25-hydroxycholesterol [2], while StarD4 binds cholesterol, 7α-hydroxycholesterol and 7-hydroperoxycholesterol [8, 9], and StarD6 binds cholesterol showing activity similar to StarD1 [10]. StarD1 and MLN64/StarD3, the closest START domain proteins to the StarD4 subfamily, have been shown to bind cholesterol [2, 11] and most recently it has been shown the ability of StarD3 to bind lutein [12]. It is worth noticing that StarD1 and MLN64/StarD3 overexpression leads to an increase in steroidogenesis [13–15] and overexpression of StarD4, StarD5, or truncated MLN64/StarD3 increase free cholesterol in membranes [2, 14, 16–18], representative evidence of their ability to move cholesterol within the cell.

The first START domain protein crystal structure reported was the C-terminal portion of human MLN64/StarD3 [11], followed subsequently by the structure of mouse StarD4 [7]. Both structures revealed similar secondary structural elements and a hydrophobic tunnel with a size consistent with the binding of one cholesterol molecule [7, 11]. Less related to the StarD4 subfamily, but also containing a START domain with a known lipid ligand, is the phosphatidylcoline transfer protein (PCTP/StarD2) [19]. StarD2 crystal structure also shows a hydrophobic tunnel, but unlike StarD1, 3, 4, and 5, selectively binds only phosphatidylcholine [20]. Modeling studies of the structure of StarD1 and MLN64 have shown that cholesterol appears to be bound by the predicted hydrophobic tunnel of both proteins. The structure also reveals changes in the loop at the entrance of the hydrophobic tunnel that may be sufficient for the uptake and release of cholesterol [21, 22].

Although the role of proteins like StarD1, PCTP/StarD2 and MLN64/StarD3 have been extensively studied [14, 18, 23][24], the role(s) of the StarD4 subfamily proteins remain uncertain. In contrast to StarD1 and MLN64/StarD3, the proteins of the StarD4 subfamily do not have N-terminal targeting sequences that should direct these proteins to specific cellular organelles. Therefore, the StarD4 subfamily of proteins are predicted to be cytoplasmic proteins, like PCTP/StarD2 [25, 26].

The tissue distribution of StarD4 is unknown. In contrast, several studies have revealed that StarD6 is expressed in the testis and nervous system [25][27–29]. StarD5 is mainly expressed in immune related cells with localization to the cytoplasm and Golgi membranes [30]. Studies in HeLa cells have suggested a diffuse cytoplasmic presence of StarD4 with some nuclear localization, as determined using a green fluorescent protein-StarD4 fusion protein [31]. Northern blotting has revealed expression of StarD4 mRNA in several tissues, including liver [7] and most recently in keratinocytes [32].

StarD5 mRNA expression is induced in response to endoplasmic reticulum (ER) stress, either in free cholesterol loaded mouse macrophages or in NIH-3T3 cells after being treated with different ER stressors [16]. In contrast, StarD4 mRNA expression is regulated by sterols through the sterol regulatory element binding protein (SREBP) pathway and in the early phase of ER stress [33].

Recent studies have demonstrated the ability of StarD4 to increase intracellular cholesteryl ester formation and bile acid synthesis following StarD4 overexpression, supporting a role for StarD4 as a cholesterol carrier to different cellular compartments, either as a facilitator of cholesterol movement within the ER or to other cholesterol carrier proteins [8]. In contrast, disruption of StarD4 expression in a newly generated StarD4 knock out mouse led only to moderate changes on weight, lipid metabolism, and bile cholesterol in the gallbladder, leading the authors to conclude that other proteins with similar functions may be able to compensate for the loss of StarD4 expression [34].

Based on current knowledge and our previous studies on StarD4, the objective of this study was to gain insight into its subcellular localization to better understand its function. StarD4 protein was expressed in 3T3-L1 mouse fibroblasts, human THP-1 macrophages, Kuppfer cells (i.e. liver macrophage equivalent), and hepatocytes. StarD4 protein expression was sterol-regulated via SREBP-2 both in 3T3-L1 cells and THP-1 macrophages. Immunocytochemistry and fractionation analysis showed that StarD4 is localized in the cytosol and the ER in 3T3-L1 cells and in THP-1 macrophages, and to move in response to cholesterol. More specifically, in THP-1 macrophages StarD4 co-localizes with ACAT-1, and was found surrounding newly forming lipid droplets. Furthermore, when pure recombinant StarD4 protein was added to an ACAT activity *in vitro* assay the rate of esterification doubled over that of controls. The observations that StarD4 is a widely expressed cholesterol carrier with sterol responsive movement and regulation coupled with its directional cholesterol movement indicates an important role for StarD4 in intracellular cholesterol transport and homeostasis.

2. MATERIALS AND METHODS

2.1 Materials

Antibodies and reagents—StarD4 polyclonal antibodies were raised in rabbits (Open Biosystems, Huntsville AL) against the human full-length StarD4 fused to GST [8]. The polyclonal antibody did not cross-react in immunoblots with the closely related StarD5 protein (data not shown). The anti-ACAT-1 monoclonal antibody and anti-Lamin B1 were purchased from Santa Cruz Biotechnologies (Santa Cruz, CA). Alexa Fluor 488-, 568-conjugated secondary antibodies, DAPI, Bodipy 493–503, and Mitotracker and Lysotracker probes were from Invitrogen (Carlsbad, CA). Anti-calnexin was purchased from Millipore (Billerica, MA). Anti-ATF6α was purchased from Imgenex (San Diego, CA). Anti-ADFP, anti-SREBP-2, anti-Aconitase-2, anti-IκB-α and anti-CD-68 antibodies were purchased from Abcam (Cambridge, MA). Oleic acid and BSA were from Sigma (Saint Louis, MO). HRP-conjugated second antibodies were purchased from BioRad (Hercules, CA). SuperSignal West Pico chemiluminiscent substrate was purchased from Pierce (Rockford, IL). Protease

inhibitor cocktail tablets were from Roche (Indianapolis, IN). Sub-cellular fractionation kit was purchased from Thermo Scientific (Rockford, IL). Fetal bovine lipoprotein-depleted serum (LPDS) was purchased from Kalen Biochemical (Montgomery Village, MD).

2.2 Methods

2.2.1 Tissues, cell cultures and treatments—Human liver sections (formalin fixed, and embedded in paraffin), human liver tissue, freshly isolated human hepatocyte suspensions, and non-parenchymal cells from human liver were provided by the Liver Tissue Procurement and Distribution System (N01-DK-9-2310). Cultured cells (3T3-L1 and THP-1 monocytes) were obtained from ATCC and grown at 37°C in 5% CO_2. 3T3-L1 cells were grown as fibroblasts-like cells and were not differentiated to adipocytes. THP-1 monocytes were differentiated to macrophages by adding 100 nM phorbol 12-myristate 13-acetate (PMA). To regulate SREBP activity, cells were treated in media with LPDS with or without the addition of sterols (10 μg/ml cholesterol, 1 μg/ml 25-hydroxycholesterol) or 20 μM mevinolin (a competitive inhibitor for HMG-CoA reductase) plus 0.5 μM mevalonate, for 20 hours.

2.2.2 RNA isolation and Real-Time Quantitative Reverse Transcription-PCR (RT-PCR)—Total RNA was isolated from cultured cells treated by using the SV Total RNA Isolation System (Promega). Two and a half micrograms of RNA was reverse transcribed in 20 μl by using oligo-dT and M-MLV Reverse Transcriptase (Invitrogen), following manufacturer's instructions. Relative quantification of SREBP-2, StarD4 and HMG CoA reductase mRNAs was performed in 20 μl reactions by using 20 ng of cDNA, forward and reverse primers at 125 nM each, and RT^2 Real Time SYBRGreen/Rox PCR master mix (SABiosciences, Frederick, MD). Primer pairs are shown in Table 1. A 7500 Fast Real-Time PCR System (Applied Biosystems, Foster City, CA) was used with the default thermal cycling profile of: 50°C for 2 min, 95°C for 10 min; 40 cycles of 95°C for 15 s, 60°C for 1 min. ROX (carboxy-X-rhodamine) was the passive reference dye for normalization. The threshold was set at 0.2 unit of normalized fluorescence. Relative standard curves were plotted for StarD4 and HMG-CoA reductase, and the mean C_t for each cDNA sample was expressed as an arbitrary value relative to standard. For each cDNA, values for StarD4, and HMG-CoA reductase were normalized to the corresponding value for GAPDH and expressed as a ratio.

2.2.3 Nuclear protein and subcellular protein fractionation isolation—For detection of SREBP-2, nuclear extracts were isolated from 3T3-L1 cells by using the NE-PER Nuclear and Cytoplasmic Extraction Reagents (Pierce). For subcellular localization of StarD4 protein, cellular fractions were isolated from 3T3-L1 cells by using the Subcellular Protein Fractionation Kit (Pierce). Isolation of the mitochondrial fraction from 3T3-L1 cells was performed as previously described [35].

2.2.4 Immunoblots—Protein samples from cultured cells and tissues were analyzed by immuno-detection using different antibodies. Briefly, samples were separated on a 12% or 8% SDS-PAGE gels and then transferred onto a PVDF membrane using a BioRad semidry transfer cell apparatus. The membrane was transferred to a blocking solution, 5% non-fat dry milk in wash buffer (1.7 mM NaH_2PO_4, 8 mM Na_2HPO_4, 145 mM NaCl, 0.1% Tween 20), at room temperature for 2 hours with shaking. The membrane was then incubated over night in 2.5% non-fat dry milk in wash buffer containing a dilution of a primary antibody at 4°C with shaking. The membrane was then washed three times in wash buffer, at room temperature for 20 min. After washing, the membrane was incubated in a 1:2000 dilution of a HRP conjugated secondary antibody at room temperature for 1 hour in a 2.5% non-fat dry milk blocking solution in PBS-wash buffer. Finally, the membrane was washed three more

times in PBS-wash buffer. Protein bands were visualized using SuperSignal West Pico Chemiluminiscent Substrate and developed on a Fuji luminescent imagining system LAS 4000. For quantitation of protein expression, bands corresponding to StarD4 from 3 independent experiments, were quantitated by densitometry using Aida Image Analyzer 2D. Values were normalized to the corresponding value for β-actin and expressed as a ratio.

2.2.5 Immunofluorescence microscopic detection of StarD4 and CD68 in liver sections—Human liver sections were deparaffinized in o-xylene, and then rehydrated by passage through a graded series of ethanol and distillated water. CD68 antigen was retrieved by heating the slides in citrate solution, pH 6.0 for 10 min. Blocking was accomplished by incubation with 10% normal goat serum and 1% BSA in PBS containing 0.05% Tween-20 for 3 hr at 22°C. For interaction with primary antibodies, sections were incubated with 5% normal goat serum in PBS/0.05% Tween-20 containing StarD4 antibody (dilution 1:400) and CD68 antibody (dilution 1:100) for 16 hr at 4°C in an incubator. After the sections were washed in PBS/0.05% Tween-20 (3×20 min), the bound primary antibodies were visualized with Alexa Fluor 488 goat anti-rabbit IgG (for StarD4), and Alexa Fluor 568 goat anti-mouse IgG (for CD68). Sections were then washed in PBS/0.05% Tween-20 (3×20 min). DNA was stained with DAPI for 5 min at room temperature, and after washing in PBS, the slides were mounted with a coverslip and viewed using a Nikon Ti-U microscope. Controls were performed in the absence of the primary antibodies or with the StarD4 pre-immune serum.

2.2.6 Immunofluorescence—Cells on overslips were washed three times with PBS and then fixed in 3.7% Formaldehyde in PBS for 10 minutes at 4°C followed by three rinses with PBS. The cells were permeabilized with 0.05% saponin in PBS for 10 minutes at 4°C followed again by three rinses with PBS. The samples were then incubated for 2 hours at room temperature with 1% BSA, 0.05% Tween 20 in PBS (buffer A). The coverslips were then incubated for 16 hours at 4°C in primary antibodies diluted in buffer A and then washed in PBS + 0.05% Tween 20. Then the coverslips were incubated for 1 hour at room temperature with fluorescent conjugated secondary antibodies (Alexa Fluor 488 goat anti-rabbit IgGs and Alexa Fluor 568 goat goat anti-rabbit IgGs for StarD4, and Alexa Fluor 568 goat anti-mouse IgGs for organelle markers and ACAT-1) diluted in buffer A. To visualize lipid droplets, the fluorophore BODIPY 493/503 which specifically stains neutral lipids, was dissolved in ethanol at 2.5 mg/ml and added to the secondary antibody solution to a final concentration of 20 μg/ml. DNA was stained with DAPI dye. The cells were viewed using a Nikon Ti-U microscope. Control experiments were performed in both cell types using pre-immune serum along with the corresponding fluorescent second antibody or just the fluorescent second antibody. In both cases a small amount of fluorescent background was observed predominantly in the nucleus of the cells (not shown).

2.2.7 ACAT activity assay—ACAT activity was determined in the microsomal fraction of mouse liver as previously described [36] in the absence or presence of StarD4 or StarD5 pure recombinant proteins in the reaction. Briefly, 16.5 pmol of StarD4 or StarD5 protein were added to the assays. After different preincubation times, [^{14}C] Oleoyl-CoA was added to the reactions, incubated for 4 minutes and stopped by adding a methanol/chloroform (2:1, vol/vol). After phases were separated the chloroform phase was dried under nitrogen and the precipitate resuspended in acetone. The reaction products were separated by thin layer chromatography in a mobile phase of hexane/ethyl acetate (9:1, vol/vol). Bands corresponding to cholesteryl esters were scraped and counted in a scintillation counter to determine ACAT activity. Units correspond to the pmol of cholesteryl esters formed per mg of microsomal protein per minute.

2.2.8 Statistics—Data from Real-Time Quantitative Reverse Transcription-PCR, immunoblots and ACAT activity *in vitro* assays are reported as means +/− S.E. of at least three separate experiments. Control and experimental groups were compared by Student's *t* test, with the threshold for significance at $p < 0.05$.

3. Results

3.1 StarD4 protein is present in liver parenchymal and non-parenchymal cells

The tissue distribution of StarD4 mRNA has previously been described [25], with liver being the tissue with the highest amounts of all the tissues analyzed. Coupled with the fact that the liver plays a central role in cholesterol metabolism, once a polyclonal antibody against the human StarD4 protein was obtained, we focused on the liver to confirm the presence of the protein. To localize this protein within the liver, immunolocalization studies on human liver sections were carried out. Figure 1A shows that hepatocytes were positive for StarD4. Also, Kupffer cells, staining with the macrophage-specific CD-68 marker, showed a strong staining for StarD4 (Fig. 1A). Of note is the absence of immunostaining of endothelial cells. Immunoreactivity was absent in liver sections incubated with preimmune serum (Fig. 1B). Immunoblot analysis of human liver extracts detected a band of approximately 25 kDa (Fig. 2). Once the expression of StarD4 in liver tissue was confirmed, we tested isolated hepatocytes and non-parenchymal cells from human liver to more closely define the expression pattern of StarD4. In contrast, we have previously shown that StarD5 protein is detected in liver only in non-parenchymal cells; more specifically within Kupffer cells [30].

Additional immunoblots were carried out on mouse samples to test the cross-reactivity of the polyclonal antibody with the mouse StarD4 protein, with positive results, showing a band slightly larger (data not shown). The difference in size between the human and mouse StarD4 proteins was expected based on the number of amino acids of each protein (205 amino acids in the case of the human protein, and 224 amino acids for the mouse protein).

3.2 StarD4 regulation in 3T3-L1 cells and THP-1 macrophages

Previous studies have shown the presence of Sterol Response Elements (SRE) on the human and mouse StarD4 promoters as well as the regulation of the gene at the mRNA level by sterols and statin treatments [16, 25]. Therefore, we wanted to confirm that StarD4 protein expression is regulated at the protein level by sterols. Two different cell types were used: 3T3-L1 cells (where previous data was reported) and THP-1 macrophages, given the important role of macrophages in cholesterol metabolism and atherosclerosis and the fact that we detected StarD4 in Kupffer cells (Fig. 1A). We used RT-PCR and immunoblots to quantify the effect of cellular sterols levels on the expression of StarD4 in 3T3-L1 cells. As expected, HMG-CoA reductase and StarD4 mRNA levels were suppressed by sterols and induced by mevinolin (Fig. 3A top panel). Also as expected, mature SREBP-2 was significantly increased when the cells were incubated with mevinolin (which depletes cellular cholesterol) and decreased when sterols were added to the media (Fig. 3A, bottom panel). Most importantly, StarD4 protein was similarly regulated (Fig. 3B). THP-1 macrophages displayed similar changes in StarD4 protein upon manipulation of cellular cholesterol levels (Fig. 4).

Recently a study showed that during the differentiation of human monocytes to macrophages SREBP-1 target genes are activated while down-regulating SREBP-2 target genes at the end of the differentiation period of six days, including StarD4 [37]. Our study shows that undifferentiated THP-1 monocytes did not express StarD4 (Fig. 5A, 0 days), but after addition of PMA to differentiate the cells to macrophages, StarD4 was expressed (Fig.

5A, days 1 to 6). We also analyzed the HMG-CoA reductase and StarD4 mRNA levels in THP-1 cells at 24 and 48 hours after addition of PMA. Figure 5B shows that after addition of PMA, THP-1 cells displayed significantly increased levels of HMG-CoA reductase, similar to levels described by Ecker *et. al.* during the first two days of the differentiation process [37], and StarD4 mRNA levels also increased. Cleaved/active SREBP-2 protein was analyzed from the nuclear fraction of the THP-1 macrophages by immunoblot (Fig. 5C) to confirm decreased expression at the end of the differentiation period. But despite the decrease of SREBP-2 in the nuclear fractions overtime, the expression of StarD4 was maintained. Therefore we decided to analyze the levels of ATF6α, a nuclear factor known to regulate StarD4 expression [33] in the macrophages over the same period of time. As also shown in Figure 5C, the levels of nuclear ATF6α were increased as monocytes differentiated to macrophages, thus giving a possible explanation to the steady levels of StarD4 in fully differentiated macrophages. Macrophage scavenger receptor 1 (MSR1) mRNA expression was used to determine macrophage differentiation (data not shown).

3.3 Subcellular localization of StarD4 in 3T3-L1 cells and THP-1 macrophages

In order to gain some insight on StarD4 function, subcellular localization studies were performed in 3T3-L1 cells and THP-1 macrophages using cellular fractionation and immunodetection approaches. First, 3T3-L1 cells cultured in complete media were immunolabeled with StarD4 antibody, which resulted in a weak and homogeneous staining as well as some punctuated staining of the cells (Fig. 6A). Upon treatment with mevinolin, the staining was greatly increased (Fig. 6B), which was expected due to higher StarD4 expression levels under the lower cellular cholesterol content that mevinolin provides. Most importantly, StarD4 appeared to move and concentrate to the peri-nuclear region of the cells, showing a reticular pattern (Fig. 6B). In order to identify the subcellular compartment where StarD4 was being localized, three different organelle specific markers were used, i.e., IκB-α, Lamin B1 and calnexin, markers for cytoplasm, nuclei and endoplasmic reticulum (ER). Only the ER marker calnexin co-localized with StarD4 when cells were cultured in the presence of mevinolin (Fig. 6C), strongly suggesting that StarD4 had moved to the ER. Furthermore, cellular fractionation of 3T3-L1 cells also showed StarD4 to be located in the cytoplasmic and membrane fractions (Fig. 6D), supporting StarD4's cytoplasmic and ER localization.

In THP-1 macrophages the immunostaining pattern for StarD4 was slightly different than the one described for 3T3-L1 cells, but still displaying a high degree of co-localization with the ER marker calnexin (not shown). Upon closer examination, the StarD4 immunostaining was clearly located around vesicles that stained positive for neutral lipids with Bodipy 493–503 (Fig. 7A). Based on this result and our earlier observations showing that StarD4 overexpression leads to an increase in cholesteryl ester formation [8], we immunostained THP-1 macrophages to detect StarD4 and ACAT-1, the enzyme responsible for cholesterol esterification and known to localize to specific ER-derived vesicles [38]. Figure 7B shows that StarD4 co-localized with ACAT-1 in many areas, more specifically around lipid vesicles.

3.4 ACAT activity assay in the presence of StarD4 and StarD5 proteins

We have previously shown that overexpression of StarD4 leads to increased esterification of cholesterol and to an increase in oil red staining of neutral lipids in cells [8]. This finding coupled with the immunocytochemistry studies described above, suggests that StarD4 could play a role in transferring free cholesterol to ACAT-enriched areas. To obtain further support for this hypothesis, we performed *in vitro* ACAT activity assays as described in the Materials and Methods section. When pure recombinant StarD4 protein was added to the assay a 2-fold increase in activity was observed compared to controls (no addition of

protein) (Fig. 8). This strongly suggests that StarD4 delivers cholesterol to the ER for esterification. To determine if this increase in cholesterol esterification was specific to StarD4, another START domain protein, StarD5, was also used. Figure 8 shows that the addition of pure recombinant StarD5 protein did not have any effect on ACAT activity, strongly suggesting that the StarD4-mediated activation of ACAT is specific.

4. Discussion

StarD4 has been characterized as a gene whose expression is regulated by sterols [16] and as a cholesterol binding protein able to distribute free cholesterol to the mitochondria and possibly to the ER [8]. In these studies we further characterize the regulation and subcellular localization of StarD4. First, we show that sterols regulate StarD4 protein levels in both 3T3-L1 cells (Fig. 3) and THP-1 macrophages (Fig. 4). We also show an additional level of regulation, as StarD4 appears to translocate within the cell in response to sterol availability (Fig. 6). Second, we show that StarD4 is closely associated with the ER and, specifically, with ER-derived vesicles enriched in ACAT-1 (Fig. 7). Furthermore, StarD4, like ACAT-1, is in close contact with lipid droplets (Fig. 7). Third, these studies also show the ability of StarD4 to increase ACAT activity (Fig. 8), indicating its ability to direct cholesterol transfer to or within the ER. In direct contrast, the closely related START domain protein 5 (StarD5) was not able to increase ACAT activity. Previously we found that StarD4 is able to stimulate cholesteryl ester formation from preformed, but not newly synthesized cholesterol, leading us to propose that StarD4 is located and functions within poorly defined compartments of the ER [8]. These studies add additional support to this hypothesis and, if confirmed, will eventually lead to a new way of explaining how highly regulated metabolically active pools of cholesterol exist and are maintained within the cell.

Immunohistochemistry and immunoblot studies showed that StarD4 is expressed in both hepatocytes and non-parenchymal cells, i.e. Kupffer cells, in the liver, the key regulatory organ in the maintenance of cholesterol metabolism. This is in clear contrast with StarD5, the closely related START domain protein, which is expressed only in Kupffer cells [2]. The presence of StarD4 in hepatocytes gives significance to previous studies that showed increased bile acid synthesis and cholesteryl ester formation following StarD4 overexpression in primary mouse hepatocytes [8].

The regulation of StarD4 expression was studied in two different models, fibroblasts and macrophages. In both mouse 3T3-L1 fibroblasts (Fig. 3A) and THP-1 macrophages (Fig. 4A), HMG-CoA reductase and StarD4 mRNAs responded to changes in the levels of sterols as previously has been described [16]. The StarD4 protein also responded in a similar fashion to that of mRNA levels (Fig. 3B and 4B). This indicates that there is no apparent sterol-mediated posttranscriptional regulation in fibroblasts, and that the levels of sterols drive the expression of StarD4.

Differentiation of THP-1 monocytes to macrophages leads to increased expression of StarD4 mRNA and protein during the first days of the differentiation period, while in monocytes the protein was undetectable (Fig. 5). This result is in line with recent work showing that differentiation of monocytes to macrophages led to increased expression of SREBP-2 target genes, including HMG-CoA reductase, during he initial period of the differentiation process to macrophages [37]. As reported by Ecker *et. al*., once the monocytes become fully differentiated macrophages after 6 days SREBP-2 and its target genes are down-regulated, while SREBP-1 and its target genes are upregulated [37]. Despite the regulation of StarD4 by SREBP-2, fully differentiated macrophages still express relatively high amounts of StarD4. A possibility is that SREBP-1 can also up-regulate StarD4, as described before in SREBP-1 transgenic mice [24], therefore the levels of StarD4 are maintained. This is not

likely since the studies by Soccio *et. al.* [16] clearly showed that StarD4 was preferentially a target gene for SREBP-2 rather than SREBP-1. In support of this thought, Ecker et al. showed that despite activation of SREBP-1 in macrophages the StarD4 gene was down-regulated [37], making it unlikely that the mechanism involved in the increased expression of StarD4 is under the control of SREBP-1. A second possibility, is that StarD4 levels are maintained in differentiated macrophages by the activation of ATF6α, as this nuclear factor has been described before to increase the expression of StarD4 [33] and we have shown (Fig. 5) that during the differentiation process the nuclear factor is activated. As an overview, macrophage differentiation from monocytes is vital to the cell abilities to handle cholesterol excess, lending credence to the importance of StarD4 in the cell cholesterol distribution, processing, export and homeostasis.

Based on our previous results in which increased expression of StarD4 in hepatocytes and macrophages led to increased levels of bile acids and cholesteryl esters [8], we decided to determine the sub-cellular localization of StarD4. In 3T3-L1 cells under normal conditions the immunostaining of StarD4 was too weak to determine its localization, but after treatment with mevinolin the presence of StarD4 in the cytosol and in the ER was evident (Fig. 6A–C). Cell fractionation studies supported the immunolocalization studies (Fig. 6D). Therefore, we speculate that under conditions of low sterols and activation of SREBP-2 target genes, including those for the uptake of cholesterol, StarD4 could act as a carrier of exogenous cholesterol to the ER. This cholesterol would be delivered to two possible places: 1) to ACAT-enriched areas of the ER for storage as cholesteryl esters; 2) to the mitochondria for the generation of oxysterols that ultimately can downregulate SREBP-2 when the required levels of cholesterol have been reached. To further explore this idea and because the accumulation of lipid droplets is not evident in 3T3-L1 cells, we also performed similar studies in THP-1 macrophages. As macrophages under normal conditions contain more StarD4 than 3T3-L1 cells, we were able to clearly determine its cytoplasmic localization and co-localization with the ER-marker calnexin (Fig. 7). Despite this similarity on the ER localization between 3T3-L1 cells and THP-1 macrophages, it was clear that the distribution was different between both models. In THP-1 macrophages the peri-nuclear localization was not evident, rendering a more disperse and punctate staining instead. Within this pattern we were also able to observe that the punctate pattern corresponded to areas of the ER associated with lipid droplets (Fig. 7A), with StarD4 probably being associated with ER areas from which lipid droplets form and bud off [39, 40]. Further evidence came from the immunolabelling of ACAT-1 together with StarD4 in THP-1 macrophages, where both proteins also co-localized in many places surrounding lipid droplets which bud off from ER-derived vesicles enriched in ACAT-1 (Fig. 7B). This would support previous observations of the existence of ER-derived vesicles enriched in ACAT [38], and the idea that StarD4 plays a role as a carrier of cholesterol from the ER to these vesicles for the esterification of cholesterol by ACAT and its storage as part of the lipid droplets.

Finally, to prove the ability of StarD4 to carry cholesterol to ACAT we performed ACAT activity *in vitro* assays. For these assays we used mouse liver microsomes with the addition of pure recombinant StarD4 or StarD5 proteins. Addition of StarD4 protein enhanced the ACAT activity by 2-fold (Fig. 8), which is similar to the increase in cholesteryl ester formation that we previously described following StarD4 overexpression in hepatocytes and macrophages [8]. This indicates that StarD4 has the ability of moving cholesterol to the proximity of the ACAT protein within the ER. More important, the fact that the addition of the closely related START domain protein 5 (StarD5), member of the StarD4 family of proteins, did not increase ACAT activity, indicates that the ability of StarD4 of carrying cholesterol, is specific to StarD4 (Fig. 8). The idea that StarD4 would play a role in the transport of cholesterol for cholesterol esterification would further support recent studies

that showed decreased cholesterol and cholesteryl esters in female StarD4 K.O. mice when challenged with a 0.5% cholesterol diet [34].

5. Conclusion

The findings of this study support the hypothesis that StarD4 plays a role in the transport of cholesterol for its esterification, indicating a central role for StarD4 in the exit of cholesterol from the ER, with important implications in the rapid distribution of cholesterol by a non-vesicular mechanism within the cells and in the control of free cholesterol levels in the ER. Therefore, StarD4 would play a role in the free cholesterol-induced ER stress and development of atherosclerosis, and potentially in the transport of cholesterol to the mitochondria to generate regulatory oxysterols.

References

1. Hylemon, P.; Pandak, W.; Vlahcevic, Z. Regulation of hepatic cholesterol homeostasis. In: Arias, IM.; Boyer, JM.; Chisari, FV.; Fausto, N.; Schachter, D.; Shafritz, editors. The Liver: Biology and Pathobiology. Lippincott Williams & Wilkins; 2001. p. 231-247.
2. Rodriguez-Agudo D, Ren S, Hylemon PB, Redford K, Natarajan R, Del Castillo A, Gil G, Pandak WM. Human StarD5, a cytosolic StAR-related lipid binding protein. Journal of lipid research. 2005; 46:1615–1623. [PubMed: 15897605]
3. Ponting CP, Aravind L. START: a lipid-binding domain in StAR, HD-ZIP and signalling proteins. Trends Biochem Sci. 1999; 24:130–132. [PubMed: 10322415]
4. Strauss JF 3rd, Kishida T, Christenson LK, Fujimoto T, Hiroi H. START domain proteins and the intracellular trafficking of cholesterol in steroidogenic cells. Mol Cell Endocrinol. 2003; 202:59–65. [PubMed: 12770731]
5. Iyer LM, Koonin EV, Aravind L. Adaptations of the helix-grip fold for ligand binding and catalysis in the START domain superfamily. Proteins. 2001; 43:134–144. [PubMed: 11276083]
6. Schultz J, Milpetz F, Bork P, Ponting CP. SMART, a simple modular architecture research tool: identification of signaling domains. Proceedings of the National Academy of Sciences of the United States of America. 1998; 95:5857–5864. [PubMed: 9600884]
7. Romanowski MJ, Soccio RE, Breslow JL, Burley SK. Crystal structure of the Mus musculus cholesterol-regulated START protein 4 (StarD4) containing a StAR-related lipid transfer domain. Proceedings of the National Academy of Sciences of the United States of America. 2002; 99:6949–6954. [PubMed: 12011453]
8. Rodriguez-Agudo D, Ren S, Wong E, Marques D, Redford K, Gil G, Hylemon P, Pandak WM. Intracellular cholesterol transporter StarD4 binds free cholesterol and increases cholesteryl ester formation. Journal of lipid research. 2008; 49:1409–1419. [PubMed: 18403318]
9. Korytowski W, Rodriguez-Agudo D, Pilat A, Girotti AW. StarD4-mediated translocation of 7-hydroperoxycholesterol to isolated mitochondria: deleterious effects and implications for steroidogenesis under oxidative stress conditions. Biochemical and biophysical research communications. 392:58–62. [PubMed: 20059974]
10. Bose HS, Whittal RM, Ran Y, Bose M, Baker BY, Miller WL. StARlike activity and molten globule behavior of StARD6, a male germ-line protein. Biochemistry. 2008; 47:2277–2288. [PubMed: 18211099]
11. Tsujishita Y, Hurley JH. Structure and lipid transport mechanism of a StAR-related domain. Nature structural biology. 2000; 7:408–414.
12. Li B, Vachali P, Frederick JM, Bernstein PS. Identification of StARD3 as a lutein-binding protein in the macula of the primate retina. Biochemistry. 2011; 50:2541–2549. [PubMed: 21322544]
13. Clark BJ, Wells J, King SR, Stocco DM. The purification, cloning, and expression of a novel luteinizing hormone-induced mitochondrial protein in MA-10 mouse Leydig tumor cells. Characterization of the steroidogenic acute regulatory protein (StAR). The Journal of biological chemistry. 1994; 269:28314–28322. [PubMed: 7961770]

14. Lin D, Sugawara T, Strauss JF 3rd, Clark BJ, Stocco DM, Saenger P, Rogol A, Miller WL. Role of steroidogenic acute regulatory protein in adrenal and gonadal steroidogenesis. Science (New York, NY). 1995; 267:1828–1831.
15. Watari H, Arakane F, Moog-Lutz C, Kallen CB, Tomasetto C, Gerton GL, Rio MC, Baker ME, Strauss JF 3rd. MLN64 contains a domain with homology to the steroidogenic acute regulatory protein (StAR) that stimulates steroidogenesis. Proceedings of the National Academy of Sciences of the United States of America. 1997; 94:8462–8467. [PubMed: 9237999]
16. Soccio RE, Adams RM, Maxwell KN, Breslow JL. Differential gene regulation of StarD4 and StarD5 cholesterol transfer proteins. Activation of StarD4 by sterol regulatory element-binding protein-2 and StarD5 by endoplasmic reticulum stress. The Journal of biological chemistry. 2005; 280:19410–19418. [PubMed: 15760897]
17. Bose HS, Baldwin MA, Miller WL. Evidence that StAR and MLN64 act on the outer mitochondrial membrane as molten globules. Endocr Res. 2000; 26:629–637. [PubMed: 11196440]
18. Moog-Lutz C, Tomasetto C, Regnier CH, Wendling C, Lutz Y, Muller D, Chenard MP, Basset P, Rio MC. MLN64 exhibits homology with the steroidogenic acute regulatory protein (STAR) and is over-expressed in human breast carcinomas. Int J Cancer. 1997; 71:183–191. [PubMed: 9139840]
19. Cohen DE, Green RM, Wu MK, Beier DR. Cloning, tissue-specific expression, gene structure and chromosomal localization of human phosphatidylcholine transfer protein. Biochimica et biophysica acta. 1999; 1447:265–270. [PubMed: 10542325]
20. Roderick SL, Chan WW, Agate DS, Olsen LR, Vetting MW, Rajashankar KR, Cohen DE. Structure of human phosphatidylcholine transfer protein in complex with its ligand. Nature structural biology. 2002; 9:507–511.
21. Mathieu AP, Fleury A, Ducharme L, Lavigne P, LeHoux JG. Insights into steroidogenic acute regulatory protein (StAR)-dependent cholesterol transfer in mitochondria: evidence from molecular modeling and structure-based thermodynamics supporting the existence of partially unfolded states of StAR. J Mol Endocrinol. 2002; 29:327–345. [PubMed: 12459035]
22. Yaworsky DC, Baker BY, Bose HS, Best KB, Jensen LB, Bell JD, Baldwin MA, Miller WL. pH-dependent Interactions of the carboxyl-terminal helix of steroidogenic acute regulatory protein with synthetic membranes. The Journal of biological chemistry. 2005; 280:2045–2054. [PubMed: 15489236]
23. Bose HS, Lingappa VR, Miller WL. Rapid regulation of steroidogenesis by mitochondrial protein import. Nature. 2002; 417:87–91. [PubMed: 11986670]
24. Horton JD, Shah NA, Warrington JA, Anderson NN, Park SW, Brown MS, Goldstein JL. Combined analysis of oligonucleotide microarray data from transgenic and knockout mice identifies direct SREBP target genes. Proceedings of the National Academy of Sciences of the United States of America. 2003; 100:12027–12032. [PubMed: 14512514]
25. Soccio RE, Adams RM, Romanowski MJ, Sehayek E, Burley SK, Breslow JL. The cholesterol-regulated StarD4 gene encodes a StAR-related lipid transfer protein with two closely related homologues, StarD5 and StarD6. Proceedings of the National Academy of Sciences of the United States of America. 2002; 99:6943–6948. [PubMed: 12011452]
26. Feng L, Chan WW, Roderick SL, Cohen DE. High-level expression and mutagenesis of recombinant human phosphatidylcholine transfer protein using a synthetic gene: evidence for a C-terminal membrane binding domain. Biochemistry. 2000; 39:15399–15409. [PubMed: 11112525]
27. Chang IY, Kim JH, Hwang G, Song PI, Song RJ, Kim JW, Yoon SP. Immunohistochemical detection of StarD6 in the rat nervous system. Neuroreport. 2007; 18:1615–1619. [PubMed: 17885612]
28. Chang IY, Kim JK, Lee SM, Kim JN, Soh J, Kim JW, Yoon SP. The changed immunoreactivity of StarD6 after pilocarpine-induced epilepsy. Neuroreport. 2009; 20:963–967. [PubMed: 19434006]
29. Gomes C, Oh SD, Kim JW, Chun SY, Lee K, Kwon HB, Soh J. Expression of the putative sterol binding protein Stard6 gene is male germ cell specific. Biology of reproduction. 2005; 72:651–658. [PubMed: 15564601]

30. Rodriguez-Agudo D, Ren S, Hylemon PB, Montanez R, Redford K, Natarajan R, Medina MA, Gil G, Pandak WM. Localization of StarD5 cholesterol binding protein. Journal of lipid research. 2006; 47:1168–1175. [PubMed: 16534142]

31. Alpy F, Tomasetto C. Give lipids a START: the StAR-related lipid transfer (START) domain in mammals. Journal of cell science. 2005; 118:2791–2801. [PubMed: 15976441]

32. Elbadawy HM, Borthwick F, Wright C, Martin PE, Graham A. Cytosolic StAR-related lipid transfer domain 4 (STARD4) protein influences keratinocyte lipid phenotype and differentiation status. Br J Dermatol. 2011; 164:628–632. [PubMed: 20969562]

33. Yamada S, Yamaguchi T, Hosoda A, Iwawaki T, Kohno K. Regulation of human STARD4 gene expression under endoplasmic reticulum stress. Biochemical and biophysical research communications. 2006; 343:1079–1085. [PubMed: 16579971]

34. Riegelhaupt JJ, Waase MP, Garbarino J, Cruz DE, Breslow JL. Targeted disruption of steroidogenic acute regulatory protein D4 leads to modest weight reduction and minor alterations in lipid metabolism. Journal of lipid research. 2010; 51:1134–1143. [PubMed: 19965609]

35. Stravitz RT, Vlahcevic ZR, Russell TL, Heizer ML, Avadhani NG, Hylemon PB. Regulation of sterol 27-hydroxylase and an alternative pathway of bile acid biosynthesis in primary cultures of rat hepatocytes. The Journal of steroid biochemistry and molecular biology. 1996; 57:337–347. [PubMed: 8639470]

36. Carr TP, Parks JS, Rudel LL. Hepatic ACAT activity in African green monkeys is highly correlated to plasma LDL cholesteryl ester enrichment and coronary artery atherosclerosis. Arterioscler Thromb. 1992; 12:1274–1283. [PubMed: 1420087]

37. Ecker J, Liebisch G, Englmaier M, Grandl M, Robenek H, Schmitz G. Induction of fatty acid synthesis is a key requirement for phagocytic differentiation of human monocytes. Proceedings of the National Academy of Sciences of the United States of America. 2010; 107:7817–7822. [PubMed: 20385828]

38. Sakashita N, Chang CC, Lei X, Fujiwara Y, Takeya M, Chang TY. Cholesterol loading in macrophages stimulates formation of ER-derived vesicles with elevated ACAT1 activity. Journal of lipid research. 2009; 51:1263–1272. [PubMed: 20460577]

39. Robenek H, Hofnagel O, Buers I, Robenek MJ, Troyer D, Severs NJ. Adipophilin-enriched domains in the ER membrane are sites of lipid droplet biogenesis. Journal of cell science. 2006; 119:4215–4224. [PubMed: 16984971]

40. Robenek H, Buers I, Hofnagel O, Robenek MJ, Troyer D, Severs NJ. Compartmentalization of proteins in lipid droplet biogenesis. Biochimica et biophysica acta. 2009; 1791:408–418. [PubMed: 19118639]

Highlights

- StarD4 is a START domain protein with a characteristic lipid binding pocket specific for cholesterol.
- StarD4 was localized in hepatocytes, macrophages and fibroblast in the cytoplasm and ER.
- StarD4 is regulated by sterol levels and its expression increased during macrophage differentiation.
- The protein is able to increase ACAT activity in an *in vitro* assay.
- The data suggest that StarD4 is a highly regulated, non-vesicular, directional, intracellular cholesterol transporter.

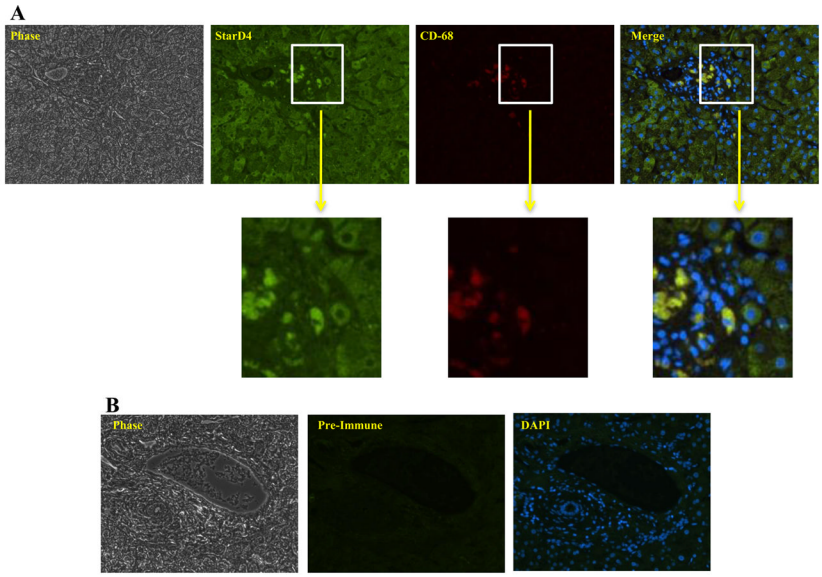

Fig. 1.

StarD4 protein is expressed in both parenchymal and Kupffer liver cels. (**A**) Liver sections were subject to immunohistochemical analysis as described in “Materials and Methods” for StarD4 (green) and CD-68 (red) at 20x magnification. Insets show high magnification views. (**B**) Negative control using pre-immune serum and nuclear staining with DAPI.

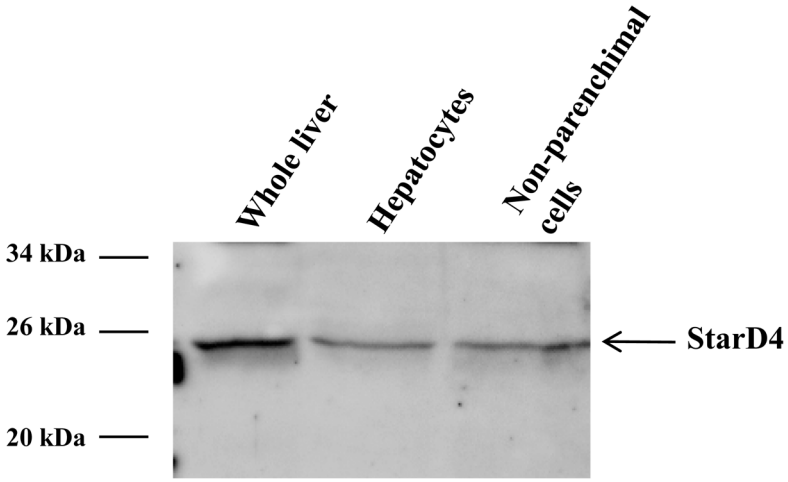

Fig. 2.

StarD4 protein is expressed in parenchymal and non-parenchymal liver cells. Whole extracts were prepared from whole human liver, freshly isolated hepatocytes, and non-parenchymal cells and analyzed by immunoblotting using the anti-StarD4 antibody as described in “Materials and Methods”.

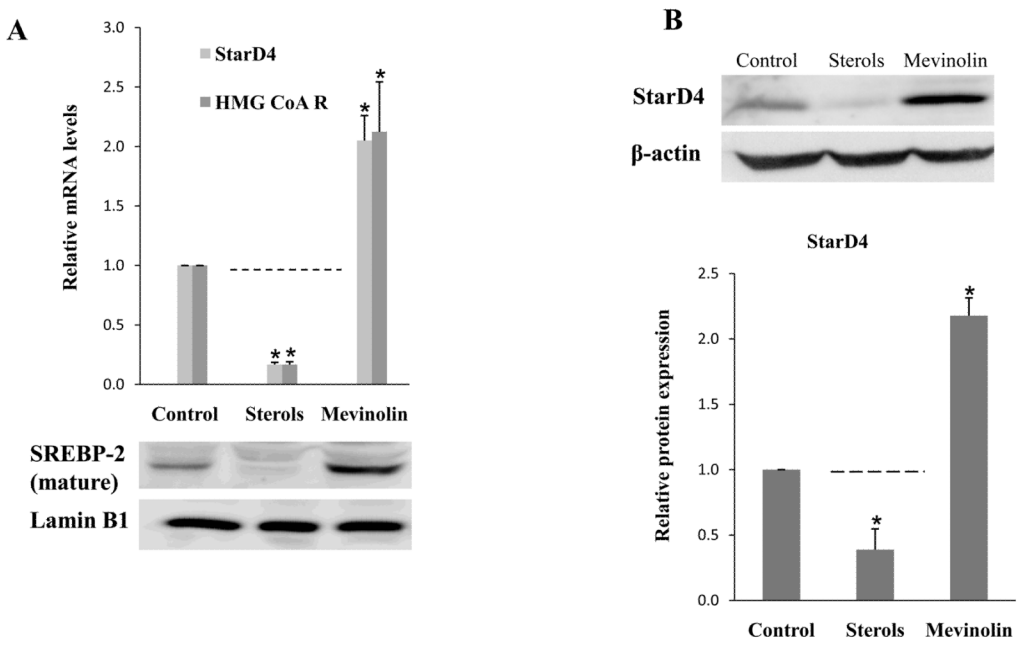

Fig. 3.

Expression of StarD4 is regulated by sterols and mevinolin in 3T3-L1 cells. **(A)** 3T3-L1 cells were cultured in LPDS-containing media with or without sterols or mevinolin as indicated and detailed in "Materials and Methods". Total RNA was prepared and StarD4 and HMG CoA reductase mRNAs quantified by quantitative RT-PCR (*upper panel*). Nuclear protein extracts were prepared from another set of cells and analyzed by immunoblotting for SREBP-2 and lamin B1, as a control, also as described in "Materials and Methods" (*lower panel*). (**B**) Whole cell extracts were prepared from another set of equally treated 3T3-L1 cells and analyzed for StarD4 and β-actin, as a control, by immunoblotting. A representative blot is shown (*upper panel*). The values represent the means ± S.D. of three experiments (*bottom panel*). *, $p < 0.05$ *versus* control cells.

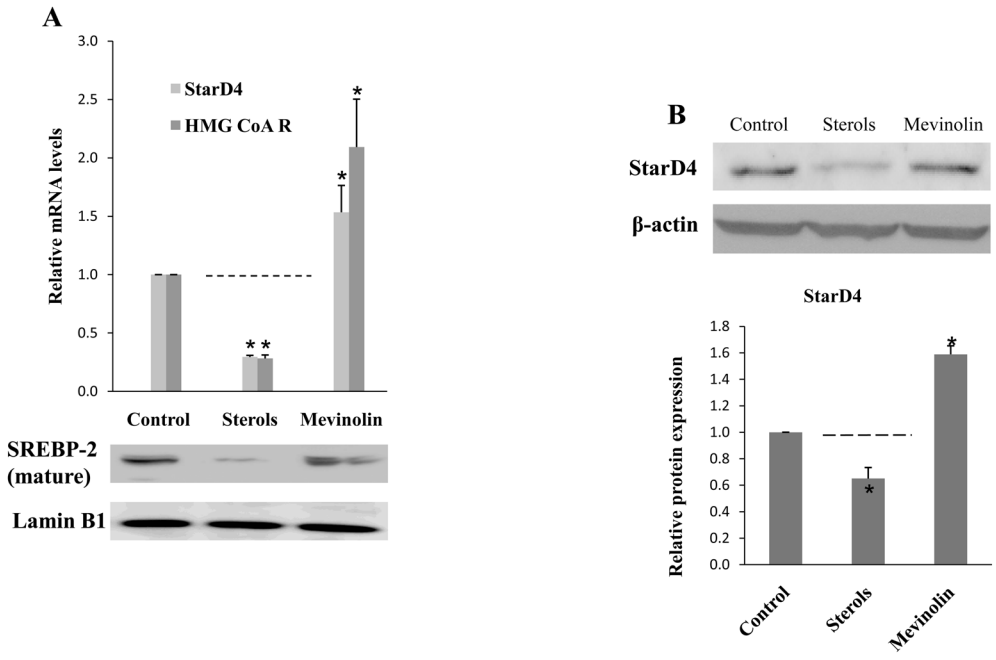

Fig. 4.

StarD4 is regulated by sterols and mevinolin in THP-1 macrophages. THP-1 macrophages were treated and analyzed as indicated in the legend for Fig. 3. **(A)** Total RNA was prepared and StarD4 and HMG CoA reductase mRNAs quantified by quantitative RT-PCR (*upper panel*). Nuclear protein extracts were prepared from another set of cells and analyzed by immunoblotting for SREBP-2 and lamin B1, as a control, also as described in "Materials and Methods" (*lower panel*). (**B**) Whole cell extracts were prepared from another set of equally treated THP-1 cells and analyzed for StarD4 and β-actin, as a control, by immunoblotting. A representative blot is shown (*upper panel*). The values represent the means ± S.D. of three experiments (*bottom panel*). *, $p < 0.05$ *versus* control cells.

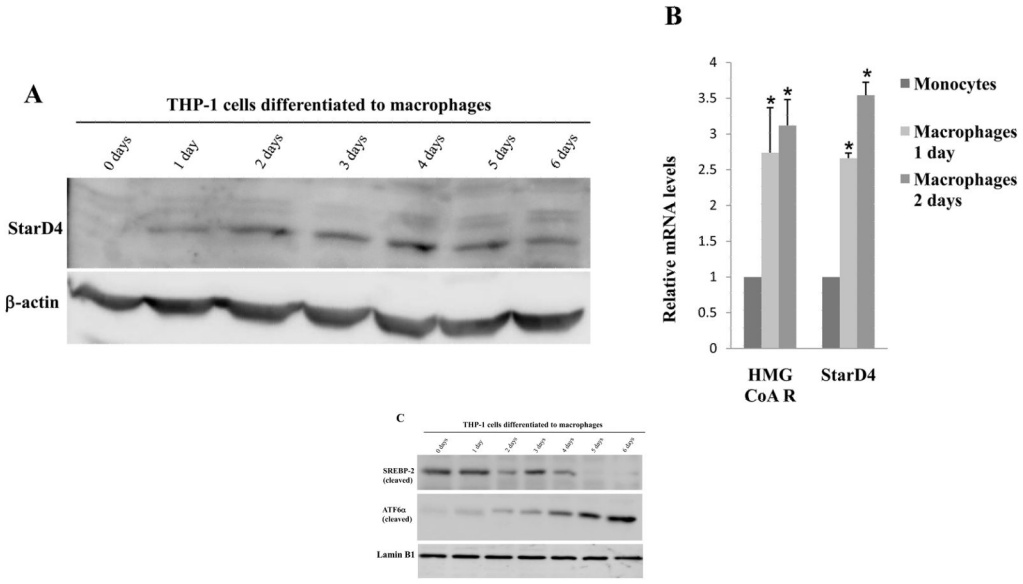

Fig. 5.

StarD4 is expressed in THP-1 cells upon differentiation to macrophages with PMA. THP-1 cells were plated and treated with PMA to induce differentiation to macrophages as explained in "Materials and Methods" over a period of 6 days. Whole cells extracts were analyzed for StarD4, and β-actin as a control by immunoblot **(A)** A representative of 3 separate experiments is shown. **(B)** Another set of THP-1 cells treated with PMA 0, 1 and 2 days were used to isolate total RNA and quantify StarD4 and HMG-CoA reductase mRNAs. The values represent the means ± S.D. of three experiments. *, $p < 0.05$ *versus* untreated cells. **(C)** Nuclear extracts from THP-1 macrophages differentiated over a period of 6 days were analyzed for SREBP-2, ATF6α and lamin B1 as a control by immunoblot.

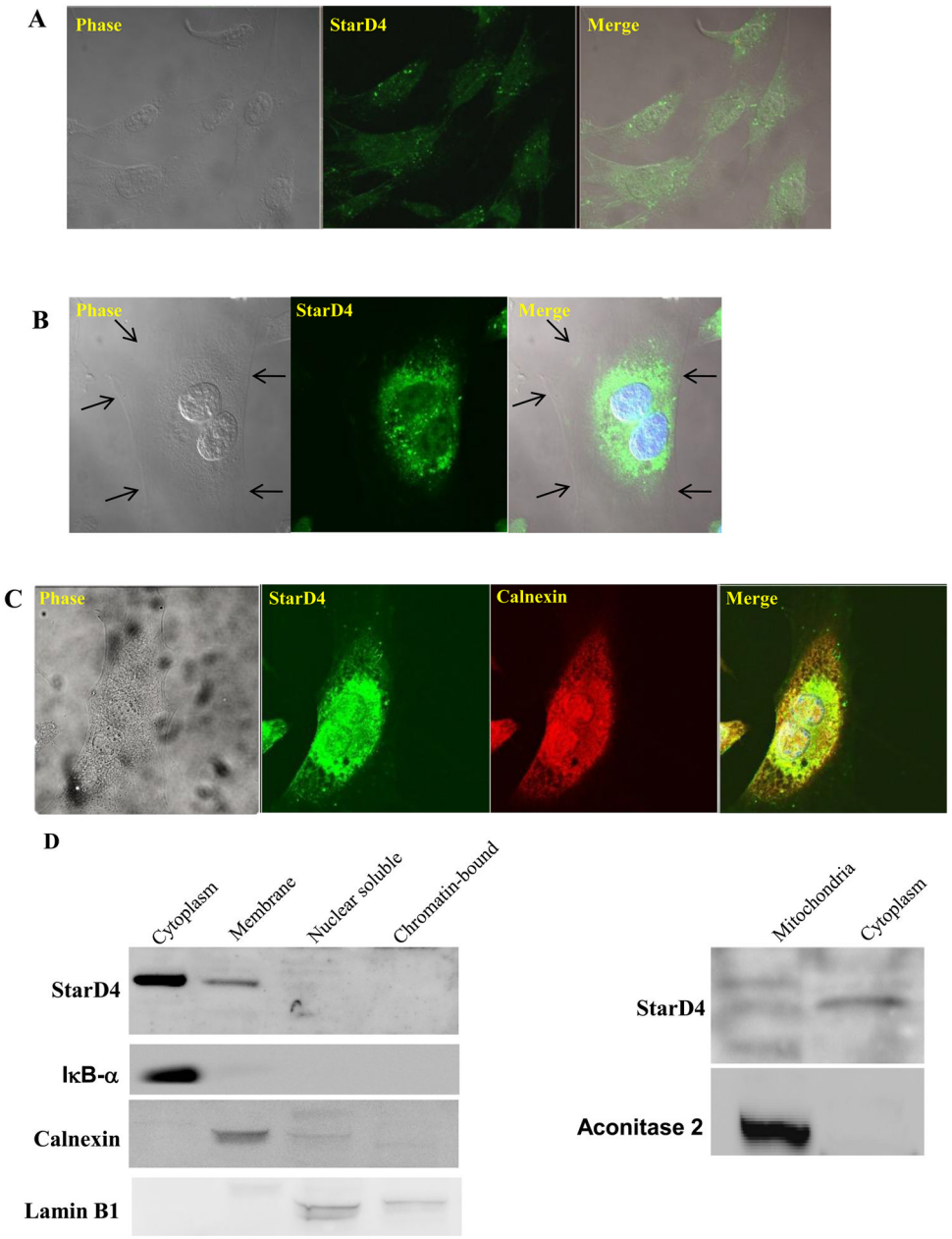

Fig. 6.

StarD4 is localized in the cytosol and ER of 3T3-L1 cells. Cells were cultured on cover slips and subject to immunocytochemical analysis for StarD4 or the ER marker calnexin as indicated, as described in "Materials and Methods". (**A**) Untreated cells (40x magnification). (**B**) and (**C**) mevinolin-treated cells (60x magnification). Merge figures 6B and 6C show blue fluorescence corresponding to DAPI staining of the nucleus. Arrows point to the cell outer membrane. (**D**) The indicated cellular fractions were prepared from mevinolin-treated cells and subjected to immunoblotting with the StarD4, IκB-α, calnexin, lamin B1 and aconitase-2 antibodies as indicated.

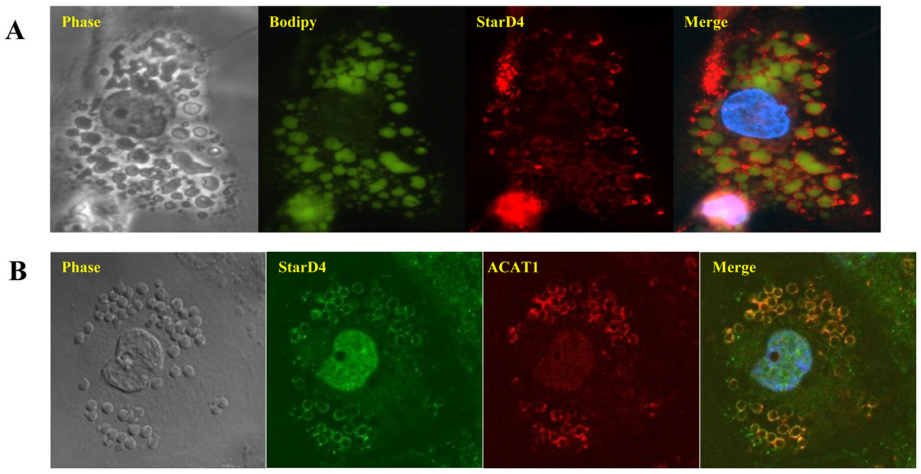

Fig. 7.

StarD4 localizes in ACAT-1-enriched ER vesicles and to surrounding lipid droplets in THP-1 macrophages. Cells were cultured on cover slips and subjected to immunocytochemical analysis for lipid droplets (Bodipy), StarD4, and ACAT-1 as indicated and described in “Materials and Methods”. In (**A**) the picture labeled as “Merge” shows the merged Bodipy, StarD4 and DAPI stained cells. In (**B**) the picture labeled as “Merge” shows the merged StarD4, ACAT1, and DAPI stained cells.

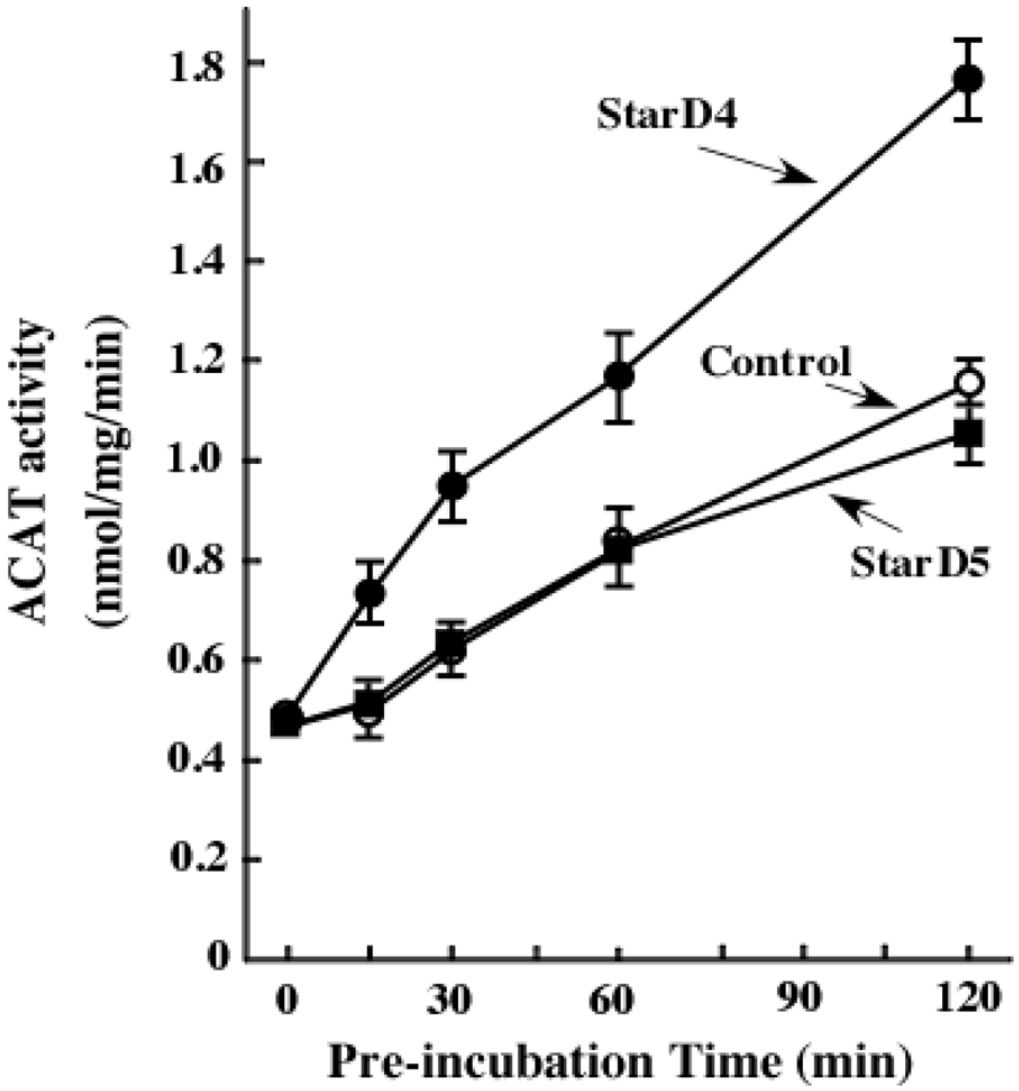

Fig. 8.

Pure recombinant StarD4 protein increases ACAT activity. 16.5 pmol of StarD4 or StarD5 protein were added to the ACAT assay reactions, and after the indicated preincubation times, [^{14}C] Oleoyl-CoA was added to the reactions, incubated for 4 minutes and stopped by adding a methanol/chloroform solution. Phases were separated and then products in the chloroform phase were separated by TLC. Bands corresponding to cholesteryl esters were localized by autoradiography, scraped and quantified in a scintillation counter to determine ACAT activity. Units correspond to the nmoles of cholesteryl esters formed per mg of microsomal protein per minute.

Table 1

Quantitative Real Time PCR oligonucleotides

Mouse: StarD4	Forward	TGTTTGGTATGGAGAGTGTGGA
	Reverse	GTCACAGCAGAGACTGACATTG
GAPDH	Forward	AGGTCGGTGTGAACGGATTTG
	Reverse	TGTAGACCATGTAGTTGAGGTCA
HMG-CoA R	Forward	AGCTTGCCCGAATTGTATGTG
	Reverse	TCTGTTGTGAACCATGTGACTTC
Human: StarD4	Forward	CAAAGCCCAAGGTGTTATAGATGAC
	Reverse	ACAGCAATTCTCTTCAAAGTTCTCC
GAPDH	Forward	TGTTGCCATCAATGACCCCCT
	Reverse	CTCCACGACGTACTCAGCG
HMG-CoA R	Forward	GGACCCCTTTGCTTAGATGAAA
	Reverse	CCACCAAGACCTATTGCTCTG